

This discussion paper is/has been under review for the journal Atmospheric Chemistry and Physics (ACP). Please refer to the corresponding final paper in ACP if available.

First detection of tidal behaviour in polar mesospheric water vapour by ground-based microwave spectroscopy

K. Hallgren and P. Hartogh

Max Planck Institute for Solar System Research, Katlenburg-Lindau, Germany

Received: 3 October 2011 – Accepted: 14 November 2011 – Published: 29 November 2011

Correspondence to: K. Hallgren (hallgren@mps.mpg.de)

Published by Copernicus Publications on behalf of the European Geosciences Union.

Tides in mesospheric water vapor

K. Hallgren and
P. Hartogh

Title Page

Abstract

Introduction

Conclusions

References

Tables

Figures

◀

▶

◀

▶

Back

Close

Full Screen / Esc

Printer-friendly Version

Interactive Discussion



Abstract

Mesospheric water vapour has been observed above ALOMAR in Northern Norway (69° N 16° E) by our group since 1995 using a 22 GHz ground-based microwave spectrometer. A new instrument with higher sensitivity, providing a much better time resolution especially in the upper mesosphere, was installed in May 2008. The time resolution is high enough to provide observations of daily variations in the water vapour mixing ratio. We present the first ground-based detections of tidal behaviour in the polar middle atmospheric water vapour distribution.

Daily variations of water vapour have been observed and due to the long chemical lifetime of water they are assumed to be caused by changing wind patterns which transport water-rich or poor air into the observed region. The detected tidal behaviour does not follow any single other dynamical field but is instead assumed to be a result of the different wind components.

Both the diurnal and semidiurnal amplitude and phase components are resolved. The former shows a stable seasonal behaviour consistent with earlier observations of wind fields and model calculations, whereas the latter appears more complex and no regular behaviour has so far been observed.

1 Introduction

The dynamical behaviour of the polar middle atmosphere is important for the global circulation and in order to correctly model it a comprehensive knowledge of all the involved processes is needed.

Atmospheric tides are known to affect the gravity waves which are an important component for the dynamical behaviour in the middle atmosphere (Fritts and Vincent, 1987; Wang and Fritts, 1991). It is therefore of interest to understand all aspects of the tidal behaviour in the Mesosphere and Lower Thermosphere (MLT) region. Tidal behaviour in temperature and the different wind components in the polar regions are

ACPD

11, 31265–31282, 2011

Tides in mesospheric water vapor

K. Hallgren and
P. Hartogh

Title Page

Abstract

Introduction

Conclusions

References

Tables

Figures

◀

▶

◀

▶

Back

Close

Full Screen / Esc

Printer-friendly Version

Interactive Discussion



Tides in mesospheric water vaporK. Hallgren and
P. Hartogh[Title Page](#)[Abstract](#)[Introduction](#)[Conclusions](#)[References](#)[Tables](#)[Figures](#)[◀](#)[▶](#)[◀](#)[▶](#)[Back](#)[Close](#)[Full Screen / Esc](#)[Printer-friendly Version](#)[Interactive Discussion](#)

commonly observed by satellite (Forbes and Wu, 2006; Manson et al., 2002a) as well as by ground-based instruments (Manson et al., 2002b; Lübken et al., 2011). A monthly mean climatology has also been published in the case of tides in the wind fields (Portnyagin et al., 2004). Measurements from satellites usually have a high temporal resolution but most of them are placed in sun-synchronous, or slowly precessing, orbits which result in a under-sampling for atmospheric tide observation purposes at any given latitude. Their global coverage is on the other hand an advantage that obviously not can be matched by ground-based instruments. The winds fields are commonly observed with MF and meteor radars which return information about the altitude range 80–100 km, and sometimes also with incoherent scatter radars which extend the altitude range to 120 km. Temperature measurements on the other hand can be done with different LIDAR techniques, but only recently were the first results for tidal observations presented (Lübken et al., 2011). In contrast to tidal behaviour in the dynamical fields, almost no information of the behaviour of atmospheric tracers such as water vapour exist – to a large extent due to the observational difficulties.

Ground-based observations of water vapour by microwave spectroscopy are a well-established technique which has proven to be useful for observations of the water vapour mixing ratio (WVMR) on different time scales, from long term trends and seasonal behaviour to isolated events such as sudden stratospheric warmings (Hartogh and Jarchow, 1995; Nedoluha et al., 1996; Seele and Hartogh, 2000; Hartogh et al., 2010). The chemical lifetime of water vapour in the middle atmosphere is longer than the typical timescales of the transport mechanisms. Thus the variability of the water vapour distribution is a direct consequence of the mean mass transport, which makes it a good tracer for the associated dynamics. Haefele et al. (2008) report observations of tidal behaviour in the WVMR measured at a mid-latitude location. Here we will present the first detections for tides in the middle atmospheric WVMR for the polar regions.

2 Instrument

To retrieve the tidal variations in the WVMR in the middle atmosphere we use a ground-based microwave spectrometer. Our observations of the polar, middle atmospheric WVMR by ground-based spectroscopy at ALOMAR (northern Norway, 69.16° N, 16.00° E) started with the successful WASPAM instrument (*Wasserdampf- und Spurengasmessungen in der Atmosphäre mit Mikrowellen*), described in Hartogh and Jarchow (1995). This instrument provided observations for some of the above mentioned papers such as (Seele and Hartogh, 2000; Sonnemann et al., 2008; Hartogh et al., 2010). A new instrument, cWASPAM (cooled-WASPAM), was installed at ALOMAR in May 2008 and has been running continuously ever since, with the exception of a few maintenance stops. It is an upgrade of the WASPAM instrument and the most notable differences are the fact that the complete front-end receiver, including antenna and calibration loads, is cooled and a polarisation splitter doubles the output. Although WASPAM also was cooled the amplifiers in cWASPAM reach lower temperatures and by cooling the complete front-end receiver the system temperature can be decreased even further. A more extensive description of the instrument can be found in Hallgren et al. (2010). Furthermore, a sister instrument called cWASPAM3 recently participated in an intercomparison campaign at Zugspitze Observatory where the stability of the instrument and good agreement to other instruments was proven (Straub et al., 2011).

The two main objectives of the new instrument was to replace the WASPAM instrument (Hartogh and Jarchow, 1995) installed 1995 and to detect and characterise the short term variations (such as tidal behaviour) of the WVMR in the polar mesosphere. By replacing WASPAM the unique long term data set of water vapour distribution attained so far is continued. Similar to its predecessor, cWASPAM observes the rotational transition of the water molecule at 22.235 GHz. The vertical and horizontal polarisation components of the signal are simultaneously analysed with two Chirp Transform Spectrometer (CTS) backends (Hartogh and Hartmann, 1990; Villanueva and Hartogh,

Tides in mesospheric water vapor

K. Hallgren and
P. Hartogh

Title Page

Abstract

Introduction

Conclusions

References

Tables

Figures

◀

▶

◀

▶

Back

Close

Full Screen / Esc

Printer-friendly Version

Interactive Discussion



Tides in mesospheric water vapor

K. Hallgren and
P. Hartogh

Title Page

Abstract

Introduction

Conclusions

References

Tables

Figures

◀

▶

◀

▶

Back

Close

Full Screen / Esc

Printer-friendly Version

Interactive Discussion



2004; Villanueva et al., 2006; Paganini and Hartogh, 2009). The CTS are identical and have a bandwidth of 40 MHz which is divided into 4096 channels with a resolution of 14 kHz each. The channels are slightly overlapping so that the effective spectral resolution becomes 10 kHz. Due to pressure broadening of the signal the narrow bandwidth
5 act as the practical lower boundary of the measurements (approximately 40–45 km). The upper limit is set by the transition altitude where the Doppler broadening becomes more important than the pressure broadening. Typical Doppler broadening of this line is ~30 kHz, well above our channel resolution. The transition for this particular line occurs at 80–85 km. Above this altitude we can no longer resolve the vertical distribution
10 of water vapour.

The noise temperature of each polarisation backend is on the order of 30 K. The spectra derived from the vertical and horizontal polarisation are statistically independent so that averaging the two signals essentially doubles the integration time, or reduces the noise by $1/\sqrt{2}$. Although the backends are identical the output differs slightly
15 due to imperfections in the polarisation splitter (an ortho-mode transducer). Hence they are averaged by the standard way of combining two independent measurements (x_1 and x_2) according to a weighting function,

$$\hat{x} = \left(\frac{1}{\sigma_1^2} + \frac{1}{\sigma_2^2} \right)^{-1} \left(\frac{x_1}{\sigma_1^2} + \frac{x_2}{\sigma_2^2} \right) \quad (1)$$

with \hat{x} as the estimate of the combined measurements. The variance of the spectral
20 noise of each spectrometer (σ_i) is used as weighting parameter. This results in the equivalent single polarisation backend with a noise temperature of approximately 20 K. Even during moderate atmospheric conditions (background temperatures ~150 K) the high sensitivity of the instrument allows retrieval of reliable atmospheric profiles up to the mesosphere every six hours. To study the dynamics in the lower range of the sensi-
25 tive region (e.g. sudden stratospheric warmings) the integration time can be shortened to four hours.

3 Data retrieval

The retrieval follows the optimal estimation method (OEM) described in Rodgers (1976). It requires temperatures of the background atmosphere which are compiled by a combination of actual weather data from NCEP (McPherson et al., 1979) and the CIRA86 model (Fleming et al., 1990). As the CIRA86 model is known to overestimate the temperatures slightly, it is modified with observations from a falling sphere climatology for ALOMAR (Lübken, 1999). In the forward model we use a linear approximation of the atmosphere with 28 layers, the lowermost located at 22.5 km and the uppermost at 92.5 km. Each layer is 2.5 km thick and no correlation between the layers is introduced mathematically (Rodgers, 1990). However, the altitude resolution of the instrument (see Fig. 1) is larger than the layer thickness in the forward model thus each layer will be affected by layers directly above and below. The OEM is a statistical method of combing two (or more) measurements in an optimal way. As the second set of measurements an estimate of a standard water vapour profile, called the a priori profile, and its associated covariance matrix, is used. This observation focuses on the short term variability and less on the absolute quantities of the water vapour and therefore a static a priori profile was used. It is a piecewise linear profile, increasing from 4 ppmv at 20 km to 7.5 ppmv at 40 km, constant with altitude up to 65 km where it starts to decrease and at 90 km there is no water left (0 ppmv). The same profile has been used for earlier work with WASPAM-data Seele and Hartogh (1999, 2000). An estimate of the quality of the data can be seen from the averaging kernels shown in Fig. (1). Averaging kernels are not expected to change significantly between subsequent measurements as long as the measurement itself have a reasonable signal to noise ratio. The kernels shown can therefore be assumed to be representative for the whole dataset.

In order to detect variabilities at short time-scales in the upper region the usual integration time of six hours is not enough. The signal is weak and it is preferred to have as many points as possible to avoid aliasing. To overcome this problem we employ

Tides in mesospheric water vapor

K. Hallgren and
P. Hartogh

Title Page

Abstract

Introduction

Conclusions

References

Tables

Figures

◀

▶

◀

▶

Back

Close

Full Screen / Esc

Printer-friendly Version

Interactive Discussion



a moving time-frame integration scheme. The initial six hour integration time is kept, but every single day in the month is added to the integration. This adds up to a total of ~180 h of integration time for the each monthly time-frame spectra. Each measurement is given a timestamp according to $T_{\text{start}} + t_{\text{int}}/2$. After the integration run the time-frame is shifted two hours – if the first data point was between 00:00 and 06:00 UT, the next one will be 02:00 and 08:00. Thus we get 12 spectra for the monthly mean 24 h period.

4 Observations and analysis

We here only present observations from one location and the source and structure of the oscillations cannot be uniquely deduced. Although we can not conclusively attribute the detected oscillations to the solar tides we have for simplicity decided to denote the 24 h period oscillation as the diurnal component and the 12 h period oscillation as semidiurnal component of the tides. To fit the observed variations a simple wave-like behaviour is assumed,

$$B + \sum A_i \cdot \cos(\omega_i + \lambda_i) \quad (2)$$

where B denotes the background water vapour mixing ratio, A_i is the amplitude, ω_i the frequency and λ_i the phase offset of the tide. Initially three components were included in the fit (diurnal, semidiurnal and terdiurnal, $i = 1, 2, 3$), however the terdiurnal component was found to be negligible and removed.

In Fig. 4 the WVMR from December 2008 for three different layers can be seen. The altitude difference between each layer (each subplot) is 10 km. The solid line is the measured variability of the WVMR as a function of the local time, and the dotted line is the fit according to Eq. (2). The chosen month for Fig. 4 is arbitrary but shows a general behaviour of the variability of the retrieved volume mixing ratio. Over the course of the year the phase and amplitude is not stable but changes. The variation of the amplitude for the diurnal component can be seen in Fig. 2 and the semidiurnal component in Fig. 3. As expected from conservation of energy the amplitude of the

Tides in mesospheric water vapor

K. Hallgren and
P. Hartogh

Title Page

Abstract

Introduction

Conclusions

References

Tables

Figures

◀

▶

◀

▶

Back

Close

Full Screen / Esc

Printer-friendly Version

Interactive Discussion



tidal waves increase as the pressure decrease with altitude. The detected amplitudes are most probably underestimated. The relatively long integration of six hours every day in the month will smooth the daily variability and hereby reduce the amplitude. Furthermore, the decreased sensitivity of the instrument at higher altitude will slightly drag the retrieved profile to the a priori profile and dampen deviations from the mean.

The amplitude of the diurnal component appears indicate a semiannual variation, with maxima during the equinox and minima during solstice. A similar, seasonal, behaviour of the diurnal tide is also noted by other groups on a global basis in wind observations from the UARS (*Upper Atmosphere Research Satellite*) (Hays et al., 1994), as well as ground-based radar observations (Vincent et al., 1988) and models (McLan-
dress, 1997). McLandress (2002a,b) explain this behaviour by tidal heating and the zonal mean winds. For the semidiurnal component (Fig. 3) the picture is different with a much more complex behaviour in the measured region. Thus a larger data-set is needed to fully isolate yearly recurring features. In general the amplitude of the diurnal component is stronger than the semidiurnal component.

The phase (not shown) of the observed tidal components changes over the course of the year, which also can be observed in wind fields presented in Portnyagin (2006). It is relatively stable with altitude which is to be expected from theoretical calculations on the wind and temperature fields, see for example Forbes (1982a,b).

In contrast to the strong seasonal variability (almost a factor of three at 70 km between summer and winter (Seele and Hartogh, 1999)) in the background levels of water vapour the absolute amplitudes of the tidal components are constant over the year.

5 Discussion

It can be seen from the averaging kernels (Fig. 1) that the atmosphere is fairly well resolved up to 80 km. Information about the water vapour above this level can only be understood as the total column depth which is projected onto the 80 km layer. This

Tides in mesospheric water vapor

K. Hallgren and
P. Hartogh

Title Page

Abstract

Introduction

Conclusions

References

Tables

Figures

◀

▶

◀

▶

Back

Close

Full Screen / Esc

Printer-friendly Version

Interactive Discussion



could explain the sometimes irregular behaviour at this altitude. It is important to note that the measured quantity is water vapour, an atmospheric tracer. At the altitudes observed water vapour has a lifetime on the order of days and longer, and we can therefore exclude any tidal influence in the water vapour production (or destruction).

5 The observed variability is therefore assumed to be caused by tidal behaviour in the transport mechanisms. Tidal behaviour has been observed in all wind fields (zonal, meridional and vertical) which implies that the resulting tidal transport vector for a tracer would be the sum of the components and as expected the observed behaviour does not follow any of the wind fields.

10 The retrieval is sensitive to changes in the temperature of the background atmosphere and oscillating temperatures could introduce artifacts in the observations. Currently, the background atmosphere used has a time-step of one day, i.e. each 24 h period is retrieved with the same background. In order to quantify the impact of unaccounted thermal oscillations a sine-like variation of the temperature was modeled and thereafter retrieved with a static background. Oscillations with an amplitude weaker
15 than ± 5 K (at 75 km) were found to be negligible. Recent LIDAR results from ALOMAR (Lübken et al., 2011) indicate thermal tides of a similar magnitude approximately 10 km higher, in the region between 85 and 96 km, which would indicate smaller amplitudes at 75 km. It should also be noted that results from GSWM-09 ((Zhang et al., 2010a,b))
20 indicate much weaker thermal tides in this region (± 1 K). We therefore assume that the unaccounted thermal tides do not introduce any large artifacts in the data. Oscillations in the background atmosphere do nevertheless introduce a certain small error in the retrieval. Thus a background atmosphere with higher time-resolution would be desirable for a better understanding of the tidal transport mechanisms in the middle atmosphere.

25 6 Conclusions

A new radiometer has been installed at ALOMAR observatory. The sensitivity has been greatly improved compared to the older WASPAM instrument, which allows for a higher

Tides in mesospheric water vapor

K. Hallgren and
P. Hartogh

Title Page

Abstract

Introduction

Conclusions

References

Tables

Figures

◀

▶

◀

▶

Back

Close

Full Screen / Esc

Printer-friendly Version

Interactive Discussion



Tides in mesospheric water vapor

K. Hallgren and
P. Hartogh

Title Page

Abstract

Introduction

Conclusions

References

Tables

Figures

◀

▶

◀

▶

Back

Close

Full Screen / Esc

Printer-friendly Version

Interactive Discussion



temporal and vertical resolution. We have looked for tidal signatures in data retrieved since May 2008 by applying a moving time-frame integration scheme. A harmonic approach with a diurnal and semidiurnal component was thereafter used in order to fit the resulting variability in water vapour levels. The observations indicates that the diurnal amplitude component in water vapour has a maximum around the equinoxes which is consistent with model predictions for tidal behaviour in winds. The fit of the semidiurnal component on the other hand is less clear and no obvious pattern could be revealed with the current dataset. In order to better understand its behaviour more data is needed.

Acknowledgements. This work was supported by the German Research Community, DFG, grant HA-3261/7-1. The authors would like to thank the staff at ALOMAR for their support in maintaining the instrument and the Atmospheric and Dynamics branch at NASA Goddard Space Center for making the NCEP data available through their automailer system.

The service charges for this open access publication have been covered by the Max Planck Society.

References

- Fleming, E. L., Chandra, S., Barnett, J., and Corney, M.: Zonal mean temperature, pressure, zonal wind and geopotential height as functions of latitude, *Advances in Space Research*, 10, 11 – 59, doi:10.1016/0273-1177(90)90386-E, 1990. 31270
- Forbes, J. M.: Atmospheric tides. I – Model description and results for the solar diurnal component., *J. Geophys. Res.*, 87, 5222–5241, doi:10.1029/JA087iA07p05222, 1982a. 31272
- Forbes, J. M.: Atmospheric tides. II – The solar and lunar semidiurnal components, *J. Geophys. Res.*, 87, 5241–5252, doi:10.1029/JA087iA07p05241, 1982b. 31272
- Forbes, J. M. and Wu, D.: Solar Tides as Revealed by Measurements of Mesosphere Temperature by the MLS Experiment on UARS., *J. Atmos. Sci.*, 63, 1776–1797, doi:10.1175/JAS3724.1, 2006. 31267
- Fritts, D. C. and Vincent, R. A.: Mesospheric momentum flux studies at Adelaide, Australia

Tides in mesospheric water vapor

K. Hallgren and
P. Hartogh

Title Page

Abstract

Introduction

Conclusions

References

Tables

Figures

◀

▶

◀

▶

Back

Close

Full Screen / Esc

Printer-friendly Version

Interactive Discussion



– Observations and a gravity wave-tidal interaction model, *J. Atmos. Sci.*, 44, 605–619, doi:10.1175/1520-0469(1987)044<0605:MMFSAA>2.0.CO;2, 1987. 31266

Haefele, A., Hocke, K., Kämpfer, N., Keckhut, P., Marchand, M., Bekki, S., Morel, B., Egorova, T., and Rozanov, E.: Diurnal changes in middle atmospheric H₂O and O₃: Observations in the Alpine region and climate models, *J. Geophys. Res. Atmos.*, 113, D17303, doi:10.1029/2008JD009892, 2008. 31267

Hallgren, K., Hartogh, P., and Jarchow, C.: A New, High-performance, Heterodyne Spectrometer for Ground-based Remote Sensing of Mesospheric Water Vapour, World Scientific Publishing Co., 19, 569–578, 2010. 31268

Hartogh, P. and Hartmann, G. K.: A high-resolution chirp transform spectrometer for microwave measurements., *Meas. Sci. Technol.*, 1, 592–595, 1990. 31268

Hartogh, P. and Jarchow, C.: Groundbased detection of middle atmospheric water vapor, in: *Global Process Monitoring and Remote Sensing of Ocean and Sea Ice*, EUROPTO-Series 2586, SPIE, Bellingham, 188–195, 1995. 31267, 31268

Hartogh, P., Sonnemann, G. R., Grygalashvily, M., Song, L., Berger, U., and Lübken, F.: Water vapor measurements at ALOMAR over a solar cycle compared with model calculations by LIMA, *J. Geophys. Res. Atmos.*, 115, D00I17, doi:10.1029/2009JD012364, 2010. 31267, 31268

Hays, P. B., Wu, D. L., and The Hrdi Science Team: Observations of the Diurnal Tide from Space., *J. Atmos. Sci.*, 51, 3077–3093, doi:10.1175/1520-0469(1994)051<3077:OOTDTF>2.0.CO;2, 1994. 31272

Lübken, F.: Thermal structure of the arctic summer mesosphere, *J. Geophys. Res.*, 104, 9135–9150, doi:10.1029/1999JD900076, 1999. 31270

Lübken, F.-J., Höffner, J., Viehl, T., Kaifler, B., and Morris, R.: First measurements of thermal tides in the summer mesopause region at Arctic and Antarctic latitudes, *Geophys. Res. Lett.*, submitted, 2011. 31267, 31273

Manson, A. H., Luo, Y., and Meek, C.: Global distributions of diurnal and semi-diurnal tides: observations from HRDI-UARS of the MLT region, *Ann. Geophys.*, 20, 1877–1890, doi:10.5194/angeo-20-1877-2002, 2002a. 31267

Manson, A. H., Meek, C., Hagan, M., Koshyk, J., Franke, S., Fritts, D., Hall, C., Hocking, W., Igarashi, K., MacDougall, J., Riggan, D., and Vincent, R.: Seasonal variations of the semi-diurnal and diurnal tides in the MLT: multi-year MF radar observations from 270 N, modelled tides (GSWM, CMAM), *Ann. Geophys.*, 20, 661-677, doi:10.5194/angeo-20-661-

Tides in mesospheric water vapor

K. Hallgren and
P. Hartogh

Title Page

Abstract

Introduction

Conclusions

References

Tables

Figures

◀

▶

◀

▶

Back

Close

Full Screen / Esc

Printer-friendly Version

Interactive Discussion



2002, 2002b. 31267

McLanress, C.: Seasonal variability of the diurnal tide: Results from the Canadian middle atmosphere general circulation model, *J. Geophys. Res.*, 102, 29747–29764, doi:10.1029/97JD02645, 1997. 31272

McLanress, C.: The Seasonal Variation of the Propagating Diurnal Tide in the Mesosphere and Lower Thermosphere. Part I: The Role of Gravity Waves and Planetary Waves., *J. Atmos. Sci.*, 59, 893–906, doi:10.1175/1520-0469(2002)059<0893:TSVOTP>2.0.CO;2, 2002a. 31272

McLanress, C.: The Seasonal Variation of the Propagating Diurnal Tide in the Mesosphere and Lower Thermosphere. Part II: The Role of Tidal Heating and Zonal Mean Winds., *J. Atmos. Sci.*, 59, 907–922, doi:10.1175/1520-0469(2002)059<0907:TSVOTP>2.0.CO;2, 2002b. 31272

McPherson, R. D., Bergman, K. H., Kistler, R. E., Rasch, G. E., and Gordon, D. S.: The NMC Operational Global Data Assimilation System, *Mon. Weather Rev.*, 107, doi:10.1175/1520-0493(1979)107<1445:TNOGDA>2.0.CO;2, 1979. 31270

Nedoluha, G. E., Bevilacqua, R. M., Michael Gomez, R., Waltman, W. B., Hicks, B. C., Thacker, D. L., and Andrew Matthews, W.: Measurements of water vapor in the middle atmosphere and implications for mesospheric transport, *J. Geophys. Res.*, 101, 21183–21194, doi:10.1029/96JD01741, 1996. 31267

Paganini, L. and Hartogh, P.: Analysis of nonlinear effects in microwave spectrometers, *J. Geophys. Res. (Atmospheres)*, 114, 13 doi:10.1029/2008JD011141, 2009. 31269

Portnyagin, Y.: A review of mesospheric and lower thermosphere models, *Adv. Space Res.*, 38, 2452–2460, doi:10.1016/j.asr.2006.04.030, 2006. 31272

Portnyagin, Y. I., Solovjova, T. V., Makarov, N. A., Merzlyakov, E. G., Manson, A. H., Meek, C. E., Hocking, W., Mitchell, N., Pancheva, D., Hoffmann, P., Singer, W., Murayama, Y., Igarashi, K., Forbes, J. M., Palo, S., Hall, C., and Nozawa, S.: Monthly mean climatology of the prevailing winds and tides in the Arctic mesosphere/lower thermosphere, *Ann. Geophys.*, 22, 3395–3410, doi:10.5194/angeo-22-3395-2004, 2004. 31267

Rodgers, C. D.: Retrieval of Atmospheric Temperature and Composition From Remote Measurements of Thermal Radiation, *Rev. Geophys. Space Phys.*, 14, 609–624, doi:10.1029/RG014i004p00609, 1976. 31270

Rodgers, C. D.: Characterization and error analysis of profiles retrieved from remote sounding measurements, *J. Geophys. Res.*, 95, 5587–5595, doi:10.1029/JD095iD05p05587, 1990.

31270

Seele, C. and Hartogh, P.: Water vapor of the polar middle atmosphere: Annual variation and summer mesosphere conditions as observed by ground-based microwave spectroscopy, *Geophys. Res. Lett.*, 26, 1517–1520, 1999. 31270, 31272

Seele, C. and Hartogh, P.: A case study on middle atmospheric water vapor transport during the February 1998 stratospheric warming, *Geophys. Res. Lett.*, 26, 3309–3312, 2000. 31267, 31268, 31270

Sonnemann, G. R., Hartogh, P., Grygalashvyly, M., Li, S., and Berger, U.: The quasi 5-day signal in the mesospheric water vapor concentration at high latitudes in 2003—a comparison between observations at ALOMAR and calculations, *J. Geophys. Res.*, 113, D04101, doi:10.1029/2007JD008875, 2008. 31268

Straub, C., Murk, A., Kämpfer, N., Golchert, S. H. W., Hochschild, G., Hallgren, K., and Hartogh, P.: ARIS-Campaign: intercomparison of three ground based 22 GHz radiometers for middle atmospheric water vapor at the Zugspitze in winter 2009, *Atmos. Meas. Tech.*, 4, 1979–1994, doi:10.5194/amt-4-1979-2011, 2011. 31268

Villanueva, G. and Hartogh, P.: The High Resolution Chirp Transform Spectrometer for the Sofia-Great Instrument, *Exp. Astron.*, 18, 77–91, doi:10.1007/s10686-005-9004-3, 2004. 31268

Villanueva, G. L., Hartogh, P., and Reindl, L.: A digital dispersive matching network for SAW devices in chirp transform spectrometers, *IEEE Transactions on Microwave Theory and Techniques*, 54, 1415–1424, doi:10.1109/TMTT.2006.871244, 2006. 31269

Vincent, R. A., Tsuda, T., and Kato, S.: A comparative study of mesospheric solar tides observed at Adelaide and Kyoto, *J. Geophys. Res.*, 93, 699–708, doi:10.1029/JD093iD01p00699, 1988. 31272

Wang, D. and Fritts, D. C.: Evidence of Gravity Wave-Tidal Interaction Observed near the Summer Mesopause at Poker Flat, Alaska., *J. Atmos. Sci.*, 48, 572–583, doi:10.1175/1520-0469(1991)048<0572:EOGWIO>2.0.CO;2, 1991. 31266

Zhang, X., Forbes, J. M., and Hagan, M. E.: Longitudinal variation of tides in the MLT region: 1. Tides driven by tropospheric net radiative heating, *J. Geophys. Res. Space Phys.*, 115, doi:10.1029/2009JA014897, 2010a. 31273

Zhang, X., Forbes, J. M., and Hagan, M. E.: Longitudinal variation of tides in the MLT region: 2. Relative effects of solar radiative and latent heating, *J. Geophys. Res. Space Phys.*, 115, doi:10.1029/2009JA014898, 2010b. 31273

Tides in mesospheric water vapor

K. Hallgren and
P. Hartogh

Title Page

Abstract

Introduction

Conclusions

References

Tables

Figures

◀

▶

◀

▶

Back

Close

Full Screen / Esc

Printer-friendly Version

Interactive Discussion



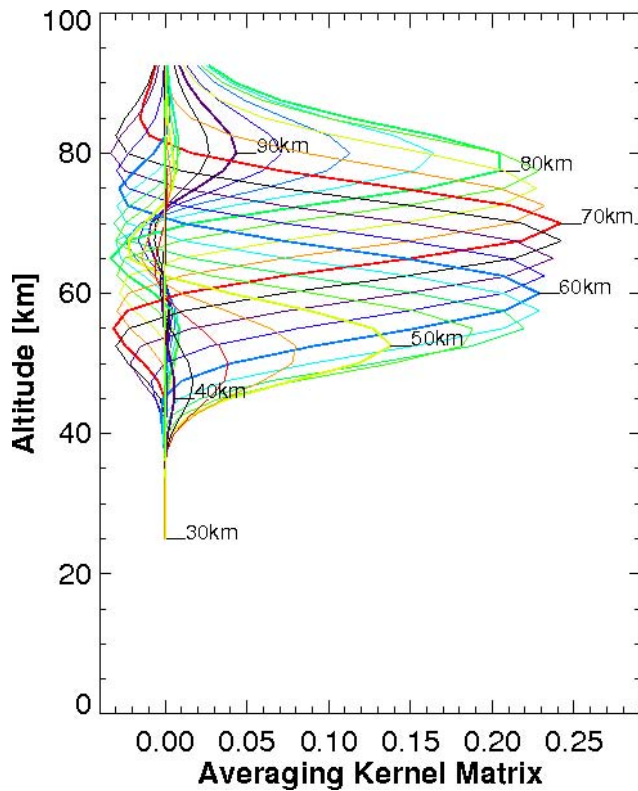


Fig. 1. Typical averaging kernels from the tidal detection mode. It can be seen that the instrument is sensitive between approximately 45 and 80 km.

Tides in mesospheric water vapor

K. Hallgren and
P. Hartogh

Title Page

Abstract

Introduction

Conclusions

References

Tables

Figures

◀

▶

◀

▶

Back

Close

Full Screen / Esc

Printer-friendly Version

Interactive Discussion



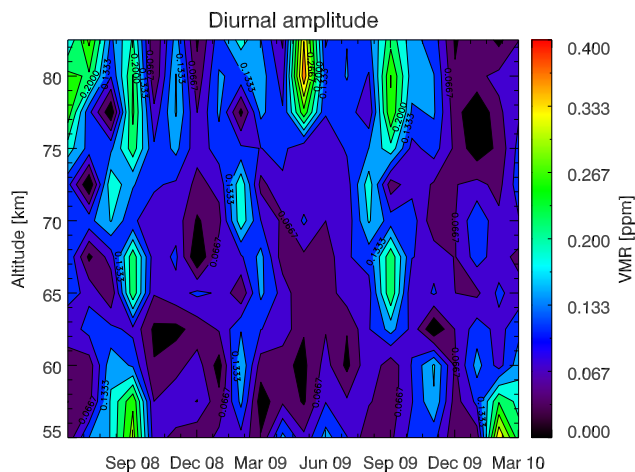
Tides in mesospheric water vaporK. Hallgren and
P. Hartogh

Fig. 2. A contour plot showing the variability over the dataset of the diurnal component of the fitted tide. Note the strong increase in the amplitude at each equinox.

Title Page

Abstract

Introduction

Conclusions

References

Tables

Figures

◀

▶

◀

▶

Back

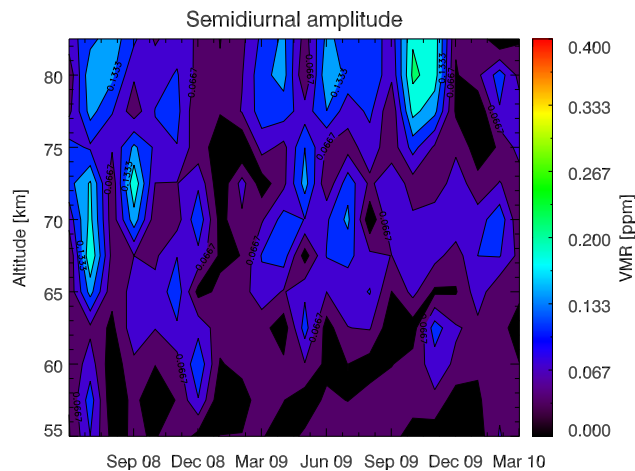
Close

Full Screen / Esc

Printer-friendly Version

Interactive Discussion



**Tides in mesospheric
water vapor**K. Hallgren and
P. Hartogh**Fig. 3.** As Fig. 2, but for the semidiurnal component.

Title Page

Abstract

Introduction

Conclusions

References

Tables

Figures

◀

▶

◀

▶

Back

Close

Full Screen / Esc

Printer-friendly Version

Interactive Discussion



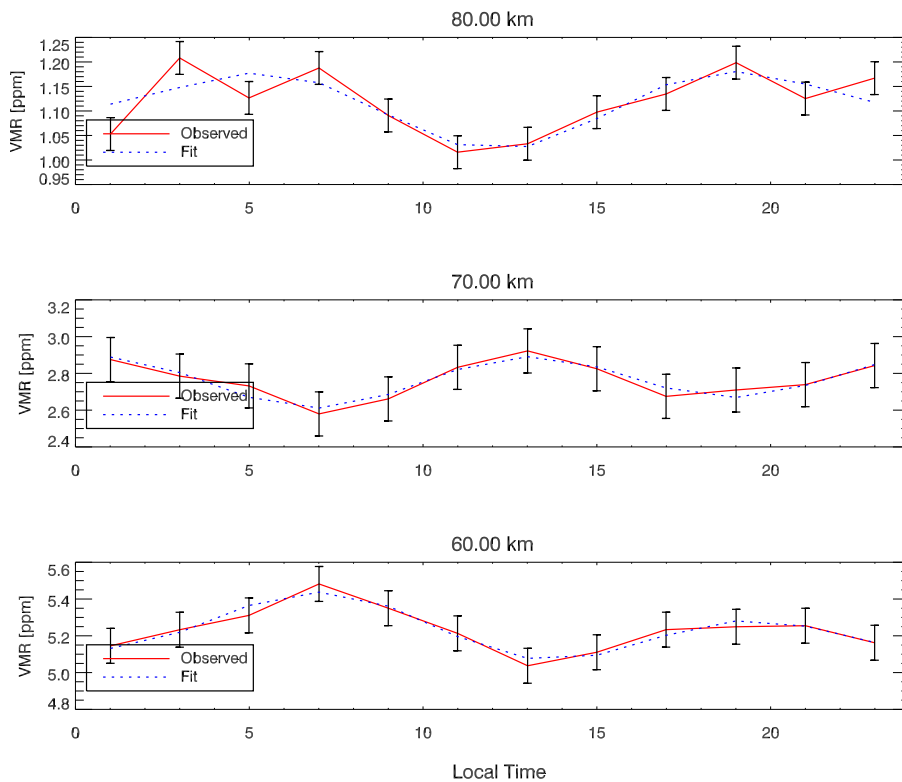
**Tides in mesospheric
water vapor**K. Hallgren and
P. Hartogh

Fig. 4. The volume mixing ratio as a function of local time for the eight topmost layers during December 2008. The vertical difference between each layer is 10 km. The solid line is the measured variability and the dotted line is the fit according to Eq. (2.)

Title Page

Abstract

Introduction

Conclusions

References

Tables

Figures

◀

▶

◀

▶

Back

Close

Full Screen / Esc

Printer-friendly Version

Interactive Discussion

